Matrix-assisted laser desorption/ionization mass spectrometry imaging of tissues via the formation of reproducible matrix crystals by fluorescence-assisted spraying method: a quantification approach

Hahm, Tae Hun
Faculty of Agriculture, Graduate School of Kyushu University

Matsui, Toshiro
Faculty of Agriculture, Graduate School of Kyushu University

Tanaka, Mitsuru
Faculty of Agriculture, Graduate School of Kyushu University

出版情報：Analytical chemistry. 94 (4), pp.1990-1998, 2022-01-18. American Chemical Society
バージョン：
権利関係：

Matrix-assisted laser desorption/ionization mass spectrometry imaging of tissues via the formation of reproducible matrix crystals by fluorescence-assisted spraying method : a quantification approach

Tae Hun Hahm,[†] Toshiro Matsui,[*,†‡] and Mitsuru Tanaka,[*,†‡]

[†]Faculty of Agriculture, Graduate School of Kyushu University, Fukuoka 819-0395, Japan

[‡]Research and Development Center for Five-Sense Devices, Kyushu University, Fukuoka 819-0395, Japan

ABSTRACT: The application of matrix-assisted laser desorption/ionization mass spectrometry (MALDI-MS) imaging to quantitative analyses is restricted by the variability of MS intensity of the analytes in nonreproducible matrix crystals of tissues. To overcome this challenge, fluorescence-assisted spraying method was developed for a constant matrix amount employing an MS-detectable fluorescent reagent, rhodamine 6G (R6G), which was sprayed with the matrix. To form a homogeneous matrix crystal on the tissue section, a matrix solution, 1,5-diaminonaphthalene (10 mg/mL), containing R6G (40 μg/mL) and *O*-dinitrobenzene (*O*-DNB, 10 mg/mL) was sprayed until the desired constant fluorescent intensity was achieved. Compared with that obtained via conventional cycle-number-fixed spraying (relative standard deviation (RSD) = 18.8%), the reproducibility of the relative MS intensity of the analyte (ferulic acid (FA), RSD = 3.1%) to R6G was significantly improved by the fluorescence-assisted matrix spraying. This result indicated that R6G could be employed as an index of the matrix amount, as well as a MS normalizing standard. The proposed matrix spraying successfully quantified nifedipine (0.5–40 pmol/mm^2 in the positive mode, R^2 = 0.965) and FA (0.5–75 pmol/mm^2 in the negative mode, R^2 = 0.9972) in the kidney section of a rat. Employing the quantitative MALDI-MS imaging assay, FA, which accumulated in the kidney of the rat after 50 mg/kg was orally administered, was visually determined to be 3.5, 3.0, and 0.2 μmol/g tissue at 15, 30, and 60 min, respectively.

The elucidation of absorption mechanisms is essential for verifying the functionalities and nutritional properties of food components and drugs. The absorption of food and drug components into the blood system, as well as accumulation in the organ, must be considered.[1–4] However, analytical methods for analyzing the microenvironments of organs are still lacking.[5] Therefore, it is necessary to establish an assay that can quantitatively and topically visualize the accumulation of absorbed compounds, including their metabolites, in targeted organs or tissue regions.

Matrix-assisted laser desorption/ionization mass spectrometry (MALDI-MS) imaging has been employed in various fields, such as food metabolism,[3-5] pharmacology,[6,7] and plant physiology,[8] because it can visualize the distribution and localization of detectable compounds in organs without employing specific labels, such as antibodies. However, MALDI-MS imaging exhibits disadvantages regarding the quantification of analytes. The factors that affect the quantitative performance of MALDI-MS imaging include matrix-to-analyte ratio,[9] inhomogeneity of tissue sections, extraction efficiency of analyte molecules,[10] inhomogenous crystallization of matrix on the tissue section,[11] variation of laser intensity,[12] ion suppression,[13] etc. In particular, the low reproducibility and inhomogeneity of matrix crystal formation during analytical runs[14] are critical issues to be solved for the improvement of the quantitative capability of MALDI-MS. Thus, highly reproducible analytical methods, such as liquid chromatography–MS (LC–MS), generally employing an internal standard (IS) that is detectable to compensate the analytical variations, are preferred in quantitative analyses.[15] Put differently, MALDI-MS imaging, which exhibits enormous advantages of simplifying the processing of samples, as well as maintaining the form of biological tissues,[16] can be a very essential analytical technique in different scientific fields if the visualized target samples can be accurately quantified. Since MALDI-MS imaging requires much less sample preparation than LC-MS (such as homogenization, extraction, purification, and column separation), it does not need to compensate the loss of analytes during the preparation. However, the fluctuation in the amount of matrix spray,[17–19] as well as the inhomogeneity of the matrix crystals on the tissue section, are serious setbacks to the quantitative ability of MALDI-MS imaging. Thus, the nondestructive evaluation of the amount of matrix spray, as well as the regulation of constant matrix spraying before MALDI irradiation, may greatly improve the quantitative ability.

Although quantitative MALDI-MS (qMALDI-MS) assays utilizing robotic matrix spotters[6,20,21] and exhibiting slight fluctuations in the matrix amount have been developed, a serious limitation persists regarding the distance between the spots (>250 μm). This limitation significantly affects the imaging quality or resolution of MS imaging. Although robotic matrix sprayers have been also developed to achieve reproducible spraying,[22] the homogeneity of matrix crystal, its distribution and amount on the tissue sections cannot be monitored and controlled. The inhomogeneity of matrix crystals is a known factor that reduces the resolution of MALDI-MS imaging.[14,23–26]

Thus, this study focused on establishing a novel quantification approach for MALDI-MS imaging by applying MS ionizable fluorescent compound and crystal-homogenizing substance as additives to the matrix solution, enabling the nondestructive monitoring of the matrix amount and enhancing the homogeneity of matrix crystal. The fluorescent compound added to matrix solution could be act as both an index of sprayed matrix amount to regulate the amount matrix sprayed before MALDI irradiation and a MS normalizing standard to compensate the variability of MS intensity of analytes due to the inhomogeneous crystallization and ionization suppression in tissue sections (Figure 1). Ferulic acid (FA), a representative absorbable bioactive food compound exhibiting anticancer effects,[27–29] and nifedipine, an

oral antihypertensive drug that accumulates in organs after oral administration,[30–32] were subjected to this qMALDI-MS imaging technique to validate its quantitative capability by comparing it with the capability of LC–MS.

EXPERIMENTAL SECTION

Materials. α-Cyano-4-hydroxycinnamic acid (CHCA) and nitrobenzene were obtained from Wako Pure Chemical Industries Ltd. (Osaka, Japan). Further, 2,5-dihydroxybenzoic acid (DHB), rhodamine 6G (R6G), 6-carboxyfluorescein, aniline, and quercetin were purchased from Sigma-Aldrich (St. Louis, MO, USA). Additionally, 1,5-diaminonaphthalene (1,5-DAN) and 7-methoxycoumarin-3-carboxylic acid were purchased from Tokyo Chemical Industry Co., Ltd. (Tokyo, Japan). *O*-Dinitrobenzene (*O*-DNB) was obtained from Nacalai Tesque Co. (Kyoto, Japan). Naphthalene was obtained from Kanto Chemical Co., Inc. (Tokyo, Japan). Sevoflurane was purchased from Maruishi Pharmaceutical Co., Ltd. (Osaka, Japan). All the reagents, which were of analytical grade, were employed without further purification.

Animal Study and Sample Collection. Eight-week-old male Sprague–Dawley (SD) rats (268.7 ± 3.9 g, SPF/VAF Crj; Charles River Japan, Kanagawa, Japan) were employed for this study. The rats were housed under the following controlled conditions: temperature, 21 ± 1 °C; humidity, 55 ± 5%; and light, twelve-hour period (from 8:00 am to 8:00 pm). After 16 h of fasting, the rats were orally administered FA (dose = 50 mg/kg). Afterward, the rats were sacrificed via exsanguination from the abdominal aorta under anesthesia employing sevoflurane. Their kidney samples were collected 0, 15, 30, and 60 min after the oral administration. The remaining blood in the organs were washed out via perfusion from the left ventricles of their hearts employing an ice-cold phosphate-buffered saline (PBS) solution (pH 7.0, 100 mL) to focus on the tissue-accumulated FA rather than the blood-accumulated ones. Thereafter, the kidney was immediately dissected and stored at −80 °C before the analyses. All the animal experiments were performed according to the Guidelines for Animal Experiments in the Faculty of Agriculture in the Graduate Course of Kyushu University and according to the Law (No. 105, 1973) and Notification (No. 6, 1980 of the Prime Minister's Office) of the Japanese Government. All the experiments were reviewed and approved by the Animal Care and Use Committee of Kyushu University (Permit Number: A20-095).

Measurement of the Fluorescent Intensity. Firstly, 7-methoxycoumarin-3-carboxylic acid, R6G, naphthalene, and 6-carboxyfluorescein were dissolved in 70% acetonitrile (ACN). Each fluorescent reagent (2–200 pmol/spot, 0.01–1 mM) was spotted onto blank kidney tissues. The fluorescence images of the spotted reagents were obtained by Fusion SOLO.7S.EDGE system (Vilber-Lourmat, Marne-la-Vallée, France) comprising blue (excitation and emission = 480 and 536 nm, respectively), green (excitation and emission = 530 and 595 nm, respectively), and red filters (excitation and emission = 640 and 750 nm, respectively). The image capture conditions included a detection time of 1.8 s. Since MALDI imaging is performed on-tissue, the average fluorescence intensity calculated from regions on the tissue sections was used to monitor the sprayed matrix amount.

Preparations of the Tissue Sections for MALDI-MS Imaging. The frozen kidney samples were sliced into 12-µm-thick sections by a CryoStar NX70 (Thermo Scientific, MA, USA) at −25 °C. The kidney sections were sequentially collected for qMALDI-MS imaging and LC–MS analysis to compare the quantitative characteristics of the two techniques. The samples for qMALDI-MS imaging were thaw-mounted on an indium–tin oxide (ITO)-coated conductive glass slide (Bruker Daltonics) and dried in a nitrogen gas flow. An ImagePrep automatic matrix sprayer was employed to spray the matrix solution, a mixture containing 1,5-DAN (10 mg/mL), *O*-DNB (10 mg/mL), and R6G (40 µg/mL) in 70% ACN, over the tissue section on the ITO glass slide under the following spraying conditions: spray power, 20%; modulation, 20%; spraying time 1.5 s; incubation time, 10 s; drying time, 60 s; and spraying cycles, 20–60. The average fluorescent intensity of the sprayed R6G (the fluorescent IS) on the tissue sections was measured by the Fusion SOLO.7S.EDGE system that was equipped with the green filter at every 1–5 cycles sequentially to regulate further spraying (until the desired constant fluorescent intensity) to obtain a constant amount of the sprayed matrix between the tissue sections, as shown in Figure 1. The average fluorescent intensity of the section was calculated by dividing the fluorescent intensity that was obtained from the kidney tissue by the number of pixels in the corresponding area of the section. The optical microscopy images were captured by an Eclipse Ts2-FL microscope (Nikon Corporation, Tokyo, Japan) with 40× to 100× resolutions before and after matrix spraying.

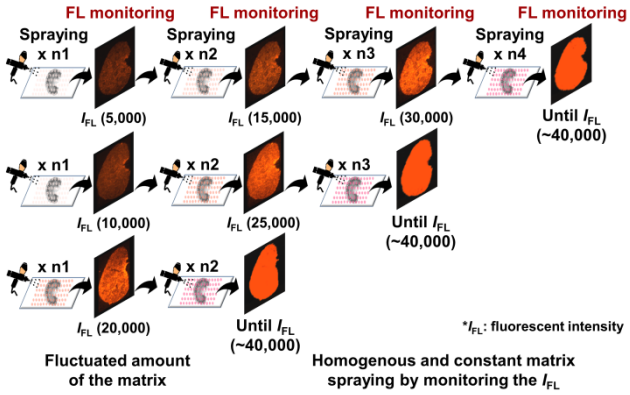

Figure 1. Scheme of the fluorescence-assisted matrix-spraying method. The matrix solution containing the fluorescent IS was homogeneously sprayed onto the sections of the kidney tissues. The homogeneity of the matrix crystal (1,5-DAN) was significantly improved by adding *O*-DNB. The average fluorescent intensity (I_{FL}) of the fluorescent IS that was sprayed on the tissue sections was measured by the Fusion SOLO.7S.EDGE system (a quick and convenient fluorescent imager) every number of cycles, either 1 or 5 cycles, up to the desired fluorescent intensity. Following the significant increase in the noise peaks that accrued from the matrix at I_{FL} = >50,000, it was further sprayed until the fluorescent intensity of ~40,000 was obtained.

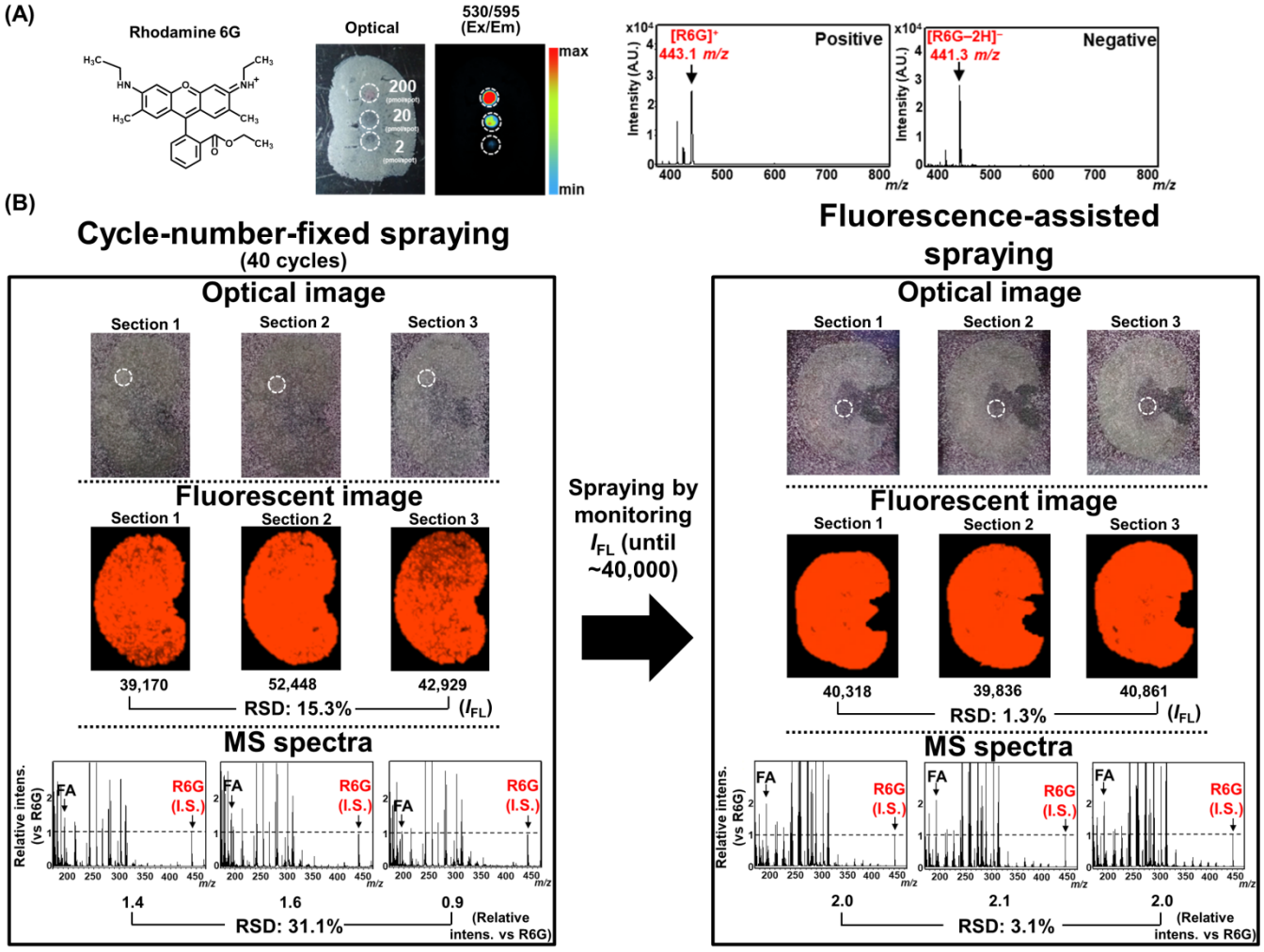

Figure 2. Fluorescence-assisted spraying method for forming reproducible matrix crystals via MALDI-MS imaging. (A) Fluorescent image of R6G obtained by the fluorescent imager employing a green filter (excitation and emission = 530 and 595 nm, respectively), and its MS spectra obtained via MALDI-MS analysis in the positive and negative detection modes utilizing 1,5-DAN as the matrix solution. (B) Optical image, fluorescent image, and MS spectra in 40 cycles of cycle-number-fixed spraying and fluorescence-assisted reproducible matrix spraying until the desired fluorescent intensity of ~40,000. MS spectra of the spotted analyte (FA; 20 pmol/spot, 0.1 mM, shown as dotted circle) were obtained for each spraying method. Additionally, the 1,5-DAN (10 mg/mL) solution containing R6G (40 μg/mL) and *O*-DNB (10 mg/mL) as the matrix additives, was sprayed on the blank kidney sections. The relative standard deviation (RSD) was calculated for the I_{FL} and relative MS intens. of FA to R6G (IS), as obtained from the ROI of the FA that was spotted on the tissue section. Sections 1, 2, and 3 exhibiting fluctuated fluorescent intensities via fixed spraying (RSD = 42.3%) were further sprayed until the desired constant fluorescent intensity to obtain a constant spray amount between the sections (RSD = 3.1%).

qMALDI-MS Imaging. The matrix-sprayed tissue sections were analyzed by an Autoflex III mass spectrometer that was equipped with a SmartBeam (Bruker Daltonics) at a spatial resolution of 100 μm. The tissue sections were subjected to MALDI-MS imaging in the positive- and negative-ion linear modes employing the following MS parameters: Ion Source 1, 20.00 kV; Ion Source 2, 18.80 kV; lens voltage, 7.50 kV; gain, 12.00; laser frequency, 200 Hz; laser power, 39%; offset, 59%; range, 20%; laser focus range, 100%; value, 6.0%; and the number of shots per pixel, 100. The ion image data were reconstructed for visualization with a mass filter of ±0.2 *m/z* employing the Bruker FlexImaging software (version 2.1). The acquired MS spectra were analyzed by the Bruker FlexAnalysis software (version 3.3) as the sum of all the spectra in the MS-imaging region. The average intensity was calculated as the sum of the spectra that were exported from the region of interest (ROI) divided by the number of pixels in the ROI (100 pixels/mm^2). Calibration curves were generated by plotting the average intensity ratio of nifedipine (2–160 pmol/0.2 μL spot) or FA (2–300 pmol/0.2 μL spot) to R6G, which was calculated with spectra from 4 mm^2 of the ROI covering the whole spot area. The weight of the tissue section (12 μm) was 430 μg/section, as calculated from the sum of the weights of three sequential tissue sections. The area of the tissue sections was

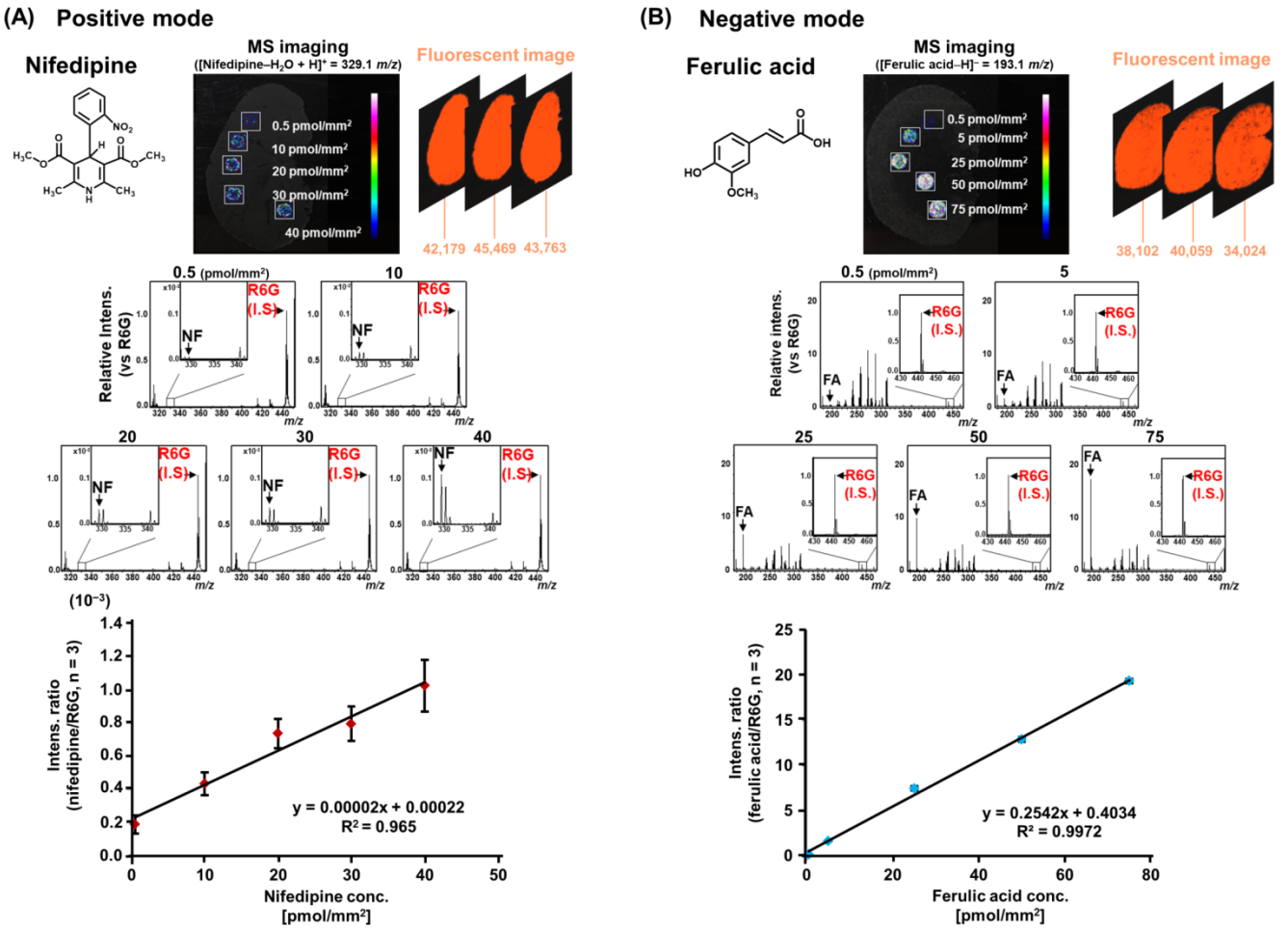

Figure 3. Calibration curves of nifedipine and FA obtained via the qMALDI-MS imaging using fluorescence-assisted matrix spraying method in the positive (A) and negative (B) modes, respectively. MS ion images of a series of spotted nifedipine ($[M–H_2O + H]^+$ = 329.1 *m/z*, 0.5–40 pmol/mm^2) and FA ($[M–H]^-$ = 193.1 *m/z*, 0.5–75 pmol/mm^2) were obtained on the blank kidney sections via positive- and negative- qMALDI-MS imaging. The fluorescent images of the positive and negative MS imaging were inserted to show the formation of the reproducible matrix crystal. The relative MS intensities of nifedipine and FA to R6G (IS) were obtained from the sum of the spectra from the ROI (4 mm^2) to cover whole spotted analytes on the kidney sections. The results were expressed as the mean ± SD of three independent tissues.

measured based on the number of pixels on the tissue section (20,411 ± 215 pixel/kidney section = 204 ± 2 mm^2/kidney section) by the FlexImaging software, which afforded the density of kidney tissue as mol/g dry tissue, to calculate the amount of FA that was accumulated in the kidney tissue. The limits of detection and quantification (LOD and LOQ) were calculated according to the equations that were reported by Sammour et al.[18]

Quantification of FA Accumulating the Kidney via LC–MS. The kidney sections of the FA-administered SD rats were lyophilized and mashed with a BioMasher II (Nippi. Inc., Tokyo, Japan). The mashed powder of five sequential kidney sections (~1.5 mg), which was adjacent to that for qMALDI-MS imaging, was homogenized with 500 µL of 50% MeOH and 0.1% formic acid containing 100 µL of 3,4-dimethoxycinnamic acid (DMCA, 1 µmol/L) as the IS by a Polytron homogenizer (KINEMATICA AG; Luzern, Switzerland; 20,000 rpm for 30 s × 3 times at 4 °C). The homogenate was subjected to sonication by a SONIFIRE 250 (Branson Ultrasonics, Emerson Japan Co., Kanagawa, Japan) at an output control of 3 for 10 s × 3 times at 4 °C. After centrifuging for 15 min at 14,000 ×*g* and 4 °C, the supernatant was ultrafiltered by an Amicon Ultra 0.5-mL 3K centrifugal filter (Millipore, Carrigtwohill, Ireland) for 30 min at 14,000 ×*g* and 4 °C. The obtained filtrate was evaporated, after which the dried filtrate was dissolved in 100 µL of a 0.1% formic acid solution. An aliquot (20 µL) of the solution was subsequently subjected to LC–time-of-flight (TOF)-MS analysis. LC–TOF/MS analysis was performed, as described in our previous study[4]. LC separation was performed employing an Agilent 1200 series system (Agilent, Waldbronn, Germany) on a Cosmosil 5C 18 AR-II column (2.0 mm I.D. × 150 mm; particle size, 5 µm; Nacalai Tesque, Kyoto, Japan) with a linear gradient elution of ACN (0–100% for >20 min) containing 0.1% formic acid at a flow rate of 0.2 mL/min at 40 °C. Electrospray ionization

Table. 1 Method validation parameters for the present qMALDI-MS imaging of ferulic acid and nifedipine

Mode	Analyte	LOD (pmol/mm^2)	LOQ (pmol/mm^2)	Intra-tissue precision of the intens. ratio, RSD (%)[a]	Inter-tissue precision of the intens. ratio, RSD (%)[a]
Positive	Nifedipine	0.35	1.07	5.1	6.9
Negative	Ferulic acid	0.12	0.36	5.4	2.5

[a]: n = 3

(ESI)–TOF/MS analysis was conducted by a microTOF II instrument (Bruker Daltonics, Bremen, Germany) in the negative mode. The ESI–TOF/MS conditions were, as follows: the drying gas (nitrogen) was employed at a flow rate of 8.0 L/min, a drying temperature of 200 °C, the nebulizing gas pressure of 1.6 bar, and a capillary voltage of 3800 V, and mass range of 100–1,000 *m/z*. All data acquisition and analyses were performed by the Bruker Data Analysis 3.2 software. An MS calibration solution containing 10 mM sodium formate in 50% ACN was injected at the beginning of each run, and all the spectra were internally calibrated. To determine the amount of FA, a calibration curve of FA, which was obtained in the blank kidney tissues under the aforementioned MS conditions, was employed: $y = 0.0994x + 7.6448$ ($R^2 = 0.9904$) [y is the peak intensity ratio (the observed peak intensity of the analyte to that of IS) and x is the concentration of FA (6–600 nmol/g dry tissue)].

RESULTS AND DISCUSSION

Constant Matrix Spraying by the MS-Detectable Fluorescent IS. The fluctuation of the amount of the matrix spray, as well as inhomogeneity of the matrix crystals on the tissue section, were serious threats to the quantitative ability of MALDI-MS imaging.[13-15] Thus, this study examined the applicability of a fluorescence probe as an IS to compensate for the variation in the amount of the matrix spray between the measurements or tissue slices. A FUSION imaging system (a simple fluorescent imager) was employed in this study to ensure quick and convenient fluorescence monitoring. As fluorescent ISs, compounds containing coumarin ($\lambda_{ex}/\lambda_{em}$ = 355/405 nm), rhodamine ($\lambda_{ex}/\lambda_{em}$ = 530/550 nm), naphthalene ($\lambda_{ex}/\lambda_{em}$ = 290/330 nm), and fluorescein ($\lambda_{ex}/\lambda_{em}$ = 490/520 nm) as their fluorophores were employed for the screening to determine the absolute quantities of IS on the surfaces of the tissues. R6G was clearly monitored on the kidney tissues (Figure 2A) via fluorescence imaging employing a green filter ($\lambda_{ex}/\lambda_{em}$ = 530/595 nm), while significant background autofluorescence, which hindered the detections of other fluorescent compounds, such as coumarin, 6-carboxyfluorescein, and naphthalene, by the red ($\lambda_{ex}/\lambda_{em}$ = 640/750 nm) or blue ($\lambda_{ex}/\lambda_{em}$ = 480/536 nm) filters, from the tissues was observed (Figure S1). Furthermore, R6G was detected via MALDI-MS in the negative- and positive ion modes employing 1,5-DAN as the matrix (Figures 2A and S2). Although R6G is known to be ionized in positive-mode LDI-MS without matrix and used as a matrix reagent for negative-mode MALDI-MS,[33–35] its detected intensity without 1,5-DAN matrix was almost negligible in the present experimental condition (at 40 µg/mL) when compared to that in MALDI-MS using 1,5-DAN (19-fold higher intensity, data not shown). Owing to the linear correlation between the fluorescence and MS intensities of R6G (R^2 = 0.9441, Figure S3), these results indicate that the fluorescent IS of R6G is a novel MS-detectable index for evaluating the matrix amount. A homogenous matrix crystal with a constant spray amount is required to improve the poor reproducibility of MALDI-MS imaging between the measurements.[14,24] Furthermore, since the homogeneity and crystal fineness of the matrix[14,36–39] are also key to improving the spatial resolution of MALDI-MS imaging,[39–41] some attempts at improving the homogeneity of matrixes via matrix additives have been reported. For instance, aniline, which forms ionic bonds with CHCA, produced fine CHCA crystals.[4] In this study, Figure S4 shows that nitrobenzene and *O*-DNB, but not aniline, at a concentration of 10 mg/mL among tested concentrations (0–10 mg/mL) in the matrix solution seemed to improve the homogeneity of the formed matrix crystal. Moreover, although co-crystallization of matrix, R6G and analyte was not confirmed, the addition of *O*-DNB, not nitrobenzene, clearly improved the homogeneity and fineness of the crystal formation of sprayed 1,5-DAN matrix (Figure S5) (average crystal diameter of sprayed droplets, 1,5-DAN only : 72 µm, nitrobenzene : 54 µm, *O*-DNB : 25 µm). Compounds containing nitro groups could be crystallized in compact crystal structures and sizes by tight and strong N–H•••O hydrogen bonds regarding the amino group.[42-44] Based on these findings, the optimized concentration of *O*-DNB (10 mg/mL) in the solution of the 1,5-DAN matrix (10 mg/mL), which exhibited the finest and most homogeneous matrix crystals, was employed for the subsequent experiments. Figure 2B shows the fluorescence images and intensities of the sprayed R6G. The average fluorescent intensity was calculated from on-tissue-regions among whole sprayed regions shown in Figure S6, since MALDI-MS imaging was performed on tissue. The fluorescent intensity varied remarkably between the sections (RSD of I_{FL} = 15.3%) even though similar optical images were obtained via 40 cycles of conventional fixed spraying for three sections that were sprayed with the 1,5-DAN solution containing R6G. Under varying matrix conditions, the relative MS intensity of FA to R6G also fluctuated in the negative mode (RSD = 31.1%). Interestingly, when the fluctuating amounts of the spray on the kidney sections were regulated until the desired constant fluorescent intensity (~40,000) was achieved based on quick fluorescent monitoring every 1–5 spraying cycles, a constant spraying amount (RSD of the I_{FL} = 1.3%) in which the reproducibility of the relative MS intensity of FA improved significantly (RSD = 3.1%), was achieved. The linear increase of MS intensity of FA by increasing matrix amount (fluorescent intensity of R6G) in Figure S7 supports the importance of constant matrix spray amount in improving the reproducibility. Moreover, Figure S8 shows that the formation of a fine crystal by *O*-DNB also improved the reproducibility of the relative MS detection of the analytes in the positive (nifedipine) and negative (FA) modes (n=5).

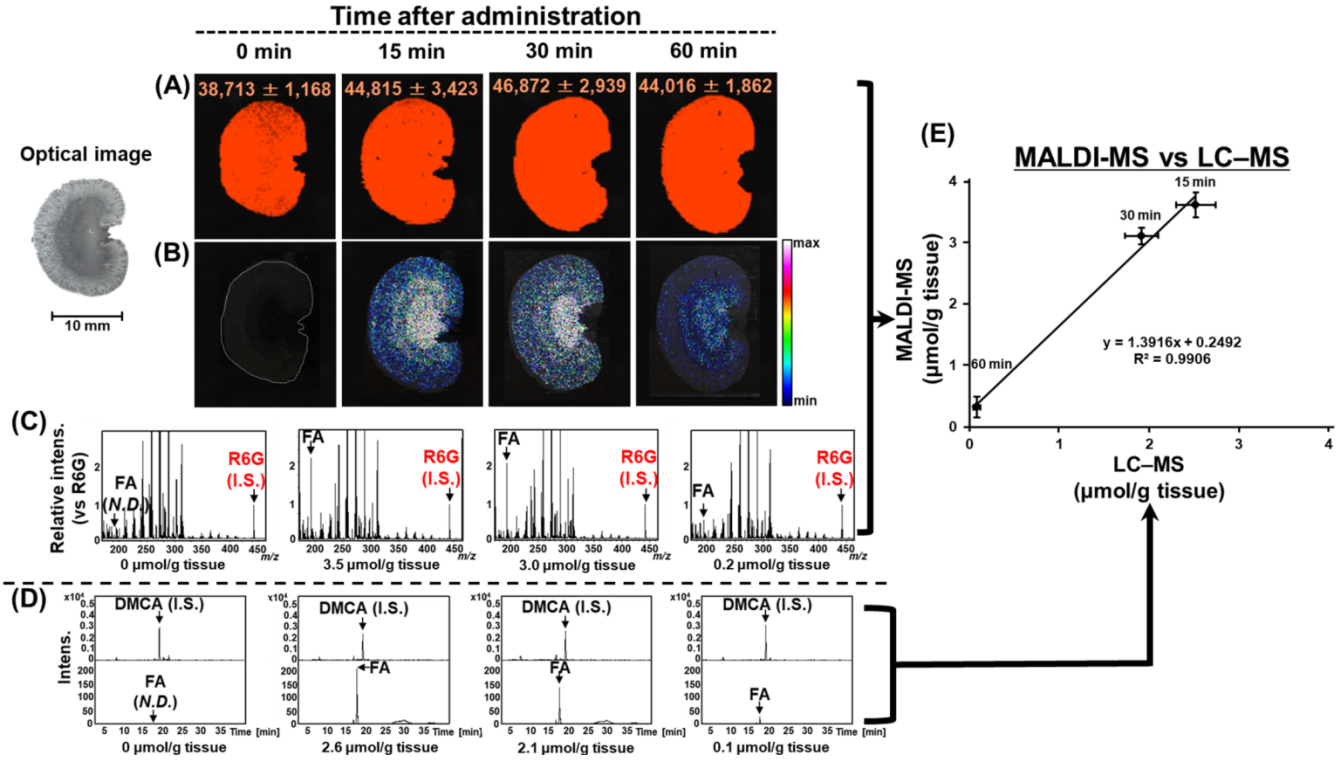

Figure 4. Quantifications of the tissue-accumulated FA in the kidneys of the rats after the administration (50 mg/kg) via LC–MS and the qMALDI-MS imaging using fluorescence-assisted spraying method. The fluorescence images (A) and corresponding MS images (B) of ferulic acid ($[M–H]^-$ = 193.1 *m/z*) are shown with the corresponding sum of the MS spectra (C) from the whole MS-imaging-analyzed tissue regions. The corresponding extracted-ion chromatograms (D) of FA (193.0527 *m/z*) and 3,4-dimethoxycinnamic acid (DMCA, 207.0657 *m/z*), the IS, of the rat kidney tissues were also demonstrated by quantitative LC–MS. The correlation curves (E) of the tissue-accumulated FA were prepared for this qMALDI-MS imaging technique and the validated LC–MS method, and the results are expressed as the mean ± SD from three independent tissues. *N.D.* indicates that there was no MS detection.

According to this result, in the present study, R6G could be defined as a spraying internal standard to act as both an index of the matrix amount and a MS normalizing standard. Thus, the formation of a fluorescence-assisted reproducible matrix by a nondestructive monitoring matrix amount before MALDI irradiation allowed the reproducible MS detection of the analytes between the measurements in this study. Moreover, since the chemical compounds R6G and *O*-DNB were developed as spraying internal standard and matrix additive to form fine crystal, respectively, these compounds are applicable not only to ImagePrep used in this study, but also to other robotic sprayers, such as TM-sprayer™, which improves reproducibility of MALDI-MS analysis.

Quantitative MALDI-MS Imaging of the Tissue-Accumulated Analytes. The quantitative capabilities of this MALDI-MS imaging using fluorescence-assisted matrix spraying were evaluated in the positive- and negative-ion modes. To validate the quantitative MALDI-MS imaging of the tissue-accumulated analytes, absorbable compounds of nifedipine[30–32] (a representative oral drug) and FA[27–29] (a representative functional food compound) were analyzed in the positive and negative modes, respectively. MS imaging in Figure 3 shows a 'coffee ring effect' of the formed crystal of nifedipine, but not FA owing to its hydrophobic characteristic,[45] which indicated that the present spraying method can maintain spatial localization of the tissue accumulated-analytes. According to these MS imaging, a linear correlation was observed in the relative MS intensities of the spotted nifedipine (0.5–40 pmol/mm^2, R^2 = 0.965) and FA (0.5–75 pmol/mm^2, R^2 = 0.9972) against R6G in the kidney sections that were subjected to a constant amount of matrix spray [fluorescent intensity, 43,803 ± 1645 (in the positive mode), 37,395 ± 3079 (in the negative mode)]. As regards the linear response of the calibration curves, it has been reported that the threshold laser fluence in MALDI depends on analyte-to-matrix molar ratio,[46] and above the threshold, MS intensities increase steeply as a power function of laser fluence.[47] Thus, the optimization of laser power along with the use of a dilution series of surrogate internal standard compensating broad changes in analyte-to-matrix molar ratio would be generally important to improve the linearity of calibration curves for qMALDI-MS assays. Although a constant laser power was applied without such a compensating approach, the obtained calibration curves exhibit an excellent linearity in the present qMALDI-MS imaging. Based on the calibration curves of nifedipine and FA, the LOD, LOQ, and inter- and intra-tissue precisions were obtained [for nifedipine: LOD, 0.35 pmol/mm^2; LOQ, 1.07 pmol/mm^2; and intra-tissue and inter-tissue RSDs, <5.1% and <6.9% (n = 3). For FA, LOD and LOQ, 0.12 and 0.36 pmol/mm^2, respectively, and intra- and inter-tissue RSDs, <5.4% and <2.5%, respectively (n = 3) (Table 1)]. Comparing the reproducibility of conventional cycle number-fixed spraying (Table S1), these validation parameters demonstrated that the proposed fluorescence-assisted matrix spraying method significantly improved

quantitative capabilities of MALDI-MS imaging. Moreover, Table S2 showed the poor linearity and reproducibility of the present data without normalization using MS intensity of R6G, which clearly demonstrated the significance of this normalization to compensate variability due to inhomogenous co-crystallization of matrix, R6G and analytes, and ionization suppression.

Quantification of the Orally Administered Rat-Kidney-Administered FA by this MALDI-MS Imaging using Fluorescence-Assisted Spraying Method. In this study, FA, which was accumulated in the organs, including the kidneys of the rats[27–29], was analyzed to validate the quantitative capability of the qMALDI-MS assay of this study. After the oral administration, the time-course accumulation behaviors of kidney-accumulated FA (0–60 min) were observed by conventional quantitative LC–MS analysis (Figures 4 and S9) after its oral administration (50 mg/kg). The kidney-section-accumulated FA was also quantified by the qMALDI-MS imaging technique of this study at a constant matrix amount with the following fluorescent intensities: 37,395 ± 3423 (0 min), 44,815 ± 3423 (15 min), 46,872 ± 2939 (30 min), 44,016 ± 3225 (60 min), utilizing adjacent sequential sections that were also utilized for the LC–MS analyses. The amount of accumulated FA, as quantified by this qMALDI-MS technique, was 1.4-folds higher than that, which was quantified by LC–MS (slope of the correlation curve = 1.3916, Figure 4). This result agrees with a previously reported one[7] in which the amount of the tissue-accumulated analyte (i.e. tetrandrine), as quantified by MALDI-MS, was higher than that, which was quantified via LC–MS. Since both qMALDI-MS and LC-MS employed the external standardization to quantify the tissue-accumulated FA, these higher values quantified by qMALDI-MS assay indicate higher extraction efficiency of tissue-accumulated FA from thin kidney tissue sections (12 μm) by qMALDI-MS than that via LC–MS. Considering the higher extraction efficiency obtained from thin tissue sections, the present quantitative MALDI-MS imaging might be applicable for different analytes and organs. Further, an advantage (facile sample preparation) of MALDI-MS imaging would also increase the extraction efficiency, thus preventing the degradation and loss of analytes via tedious preparation processes, as observed in LC–MS. Notably, a significant linear correlation was observed between this qMALDI-MS imaging technique and LC–MS employing the time-course accumulation of FA in the kidney tissues of the rats ($R^2 = 0.9906$, n = 3, Figure 4). To date, the quantitative performance of the MALDI-MS imaging technique by Chumbley et al.[6] who employed isotope-labeled ISs and a robotic spotter, is the best (RSD = 11.4%). However, their micro-spotting method was limited by the spot distance (>250 μm), whereas this qMALDI-MS imaging using fluorescence-assisted spraying method might be key owing to the application of matrix spraying, which can achieve high-resolution MS imaging (spatial resolution = >10 μm).[48–50] Moreover, considering the application of the present chemical improvement in the uniformity of matrix amount, and homogeneity of matrix crystals, quantitative MALDI-MS imaging at micron level resolution might be achieved using advanced matrix spraying devices.[51,52] Figure S10 shows that this qMALDI-MS imaging could quantify the amount of tissue-accumulated FA and visualize its specific localization. For example, FA in the pelvis, medulla, and cortex regions were quantified after 15 min of administration as 18.5, 4.9, and 1.3 μmol/g tissue, respectively, assuming that the density of the whole kidney section was homogeneous. Moreover, the accumulated amount decreased with time after the administration. For instance, the pelvis-specific accumulations of FA were 18.5, 11.5, and 1.5 μmol/g tissue in 15, 30, and 60 min, respectively (Figure S10). These findings demonstrate that this qMALDI-MS imaging using fluorescence-assisted spraying method can quantify the regional accumulation of analytes.

CONCLUSIONS

A quantitative approach of performing MALDI-MS imaging in tissue sections via fluorescence-assisted constant matrix spraying was established to enable the quantification of tissue-accumulated analytes, as well as the visualization of their spatial localization, with a good spatial resolution. Successful quantitative and reproducible capabilities were achieved via the formation of fluorescence-assisted reproducible matrix crystals by R6G (the IS) in the 1,5-DAN solution containing *O*-DNB before MALDI irradiation. This qMALDI-MS imaging approach could reveal the quantitative distribution of analytes in the microenvironments of different biological tissues, thereby availing a valuable analytical tool for evaluating the bioavailabilities and mechanisms of bioactive compounds in different application fields, such as medical, pharmaceutical, and functional food sciences.

ASSOCIATED CONTENT

Supporting Information

The following Supporting Information is available free of charge on the ACS Publications website.

Fluorescence observation images of the different candidates for fluorescent IS; MALDI-MS analysis results of R6G employing four different matrix solutions; A linear correlation between fluorescent intensity and MS intensity of R6G in a range of fluorescent intensity between 20,000–60,000; Optimization of the concentration of additives (such as aniline, nitrobenzene, and *O*-DNB) for the formation of a homogenous crystal with 1,5-DAN; Homogeneities of the matrix crystals of 1.5-DAN containing different additives (such as nitrobenzene and *O*-DNB); Optical and fluorescent images (shown as 3D mode) of rat kidney section sprayed with 1,5-DAN (10 mg/mL) containing R6G (40 μg/mL) and *O*-DNB (10 mg/mL) as the matrix additives; Linear correlation between MS intensity of FA and matrix amount (fluorescent intensity of R6G); Reproducibility of the MALDI-MS imaging using fluorescence-assisted matrix spraying with or without *O*-DNB; LC–MS time-course quantification of the accumulated ferulic acid in the kidneys of the rats after the administration; Regional quantification of the accumulated ferulic acid in the kidneys of the rats; Method validation parameters for the qMALDI-MS imaging using conventional spraying method (40 cycles); Method validation parameters for the present qMALDI-MS imaging of ferulic acid and nifedipine without normalization using MS intensity of R6G

AUTHOR INFORMATION

Corresponding Authors

* E-mail: mitsurut@agr.kyushu-u.ac.jp (M.Tanaka.)
* E-mail: tmatsui@agr.kyushu-u.ac.jp (T.Matsui.)

Present Addresses

†Faculty of Agriculture, Graduate School of Kyushu University, Fukuoka 819-0395, Japan

‡Research and Development Center for Five-Sense Devices, Kyushu University, Fukuoka 819-0395, Japan

Author Contributions

T.H. Hahm, M. Tanaka, and T. Matsui designed the experiments. T.H. Hahm and M. Tanaka performed the animal experiments. T.H. Hahm prepared the tissue sections. T.H. Hahm performed the MALDI-MS imaging and fluorescence imaging experiments. T.H. Hahm and M.Tanaka analyzed the obtained data and drafted the manuscript. T. Matsui supervised the manuscript. All the authors contributed meaningful feedback for the project and manuscript.

Notes:

The authors declare no competing financial interest.

ACKNOWLEDGMENT

This work was partly supported by JSPS KAKENHI (Grant Numbers JP21H03798 (M.T.) and JP21H05006 (T.M.), a Lotte Research Promotion Grant to M. T., and a Qdai-jump Research Program Grant to M.T. The authors thank the Center for Advanced Instrumental and Educational Supports of the Faculty of Agriculture (Kyushu University) for the technical support on cryosectioning and fluorescence imaging.

REFERENCES

(1) Welling, P. Influence of Food and Diet on Gastrointestinal Drug Absorption: A Review. *J. Pharmacokinet. Biopharm.* **1977**, *5*, 291–334.
(2) Ávila-Gálvez, M.; García-Villalba, R.; Martínez-Díaz, F.; Ocaña-Castillo, B.; Monedero-Saiz, T.; Torrecillas-Sánchez, A.; Abellán, B.; González-Sarrías, A.; Espín. J. Metabolic Profiling of Dietary Polyphenols and Methylxanthines in Normal and Malignant Mammary Tissues from Breast Cancer Patients. *Mol. Nutr. Food Res.* **2019**, *63*, 1801239.
(3) Hahm, T. H.; Tanaka, M.; Nguyen, H. N.; Tsutsumi, A.; Aizawa, K.; Matsui, T. Matrix-Assisted Laser Desorption/Ionization Mass Spectrometry-Guided Visualization Analysis of Intestinal Absorption of Acylated Anthocyanins in Sprague-Dawley Rats. *Food Chem*. **2021**, *334*, 127586.
(4) Tanaka, M; Dohgu, X.; Komabayashi, G.; Kiyohara, H.; Takata, F.; Kataoka, Y.; Nirasawa, T.; Maebuchi, M.; Matsui T. Brain-Transportable Dipeptides across the Blood-Brain Barrier in Mice. *Sci. Rep.* **2019**, *9*, 5769.
(5) Nguyen, H. N.; Tanaka, M.; Li, B.; Ueno, T.; Matsuda, H.; Matsui, T. Novel *in situ* Visualisation of Rat Intestinal Absorption of Polyphenols via Matrix-Assisted Laser Desorption/Ionisation Mass Spectrometry Imaging. *Sci. Rep.* **2019**, *9*, 3166.
(6) Chumbley, C. W.; Reyzer, M. L.; Allen, J. L.; Marriner, G. A.; Via, L. E.; Barry, C. E.; Caprioli, R. M. Absolute Quantitative MALDI Imaging Mass Spectrometry: A Case of Rifampicin in Liver Tissues. *Anal. Chem.* **2016**, *88*, 2392–2398.
(7) Tang, W.; Chen, J.; Zhou, J.; Ge, J.; Zhang, Y.; Li, P.; Li. B. Quantitative MALDI Imaging of Spatial Distributions and Dynamic Changes of Tetrandrine in Multiple Organs of Rats. *Theranostics*, **2019**, *9*, 932–944.
(8) Shiono, K.; Hashizaki, R.; Nakanishi, T.; Sakai, T.; Yamamoto, T.; Ogata, K.; Harada, K.; Ohtani, H.; Katano, H.; Taira, S. Multi-Imaging of Cytokinin and Abscisic Acid on the Roots of Rice (Oryza sativa) Using Matrix-Assisted Laser Desorption/Ionization Mass Spectrometry. *J. Agric. Food Chem.* **2017**, *65*, 7624−7628.
(9) Yao, J.; Scott, J. R.; Young, M. K.; Wilkins, C. L. Importance of Matrix: Analyte Ratio for Buffer Tolerance using 2,5-Dihydroxybenzoic Acid as A Matrix in Matrix-Assisted Laser Desorption/Ionization-Fourier Transform Mass Spectrometry and Matrix-Assisted Laser Desorption/Ionization-Time of Flight. *J. Am. Soc. Mass Spectrom.* **1998**, *9*, 805–813.
(10) Unsihuay, D.; Sanchez, D. M.; Laskin, J. Quantitative Mass Spectrometry Imaging of Biological Systems. *Annu. Rev. Phys. Chem.* **2021**, *72*, 307-329.
(11) Hanton, S.D.; Clark, P. A. C.; Owens, K. G.; Investigations of Matrix-Assisted Laser Desorption/Ionization Sample Preparation by Time-of-Flight Secondary Ion Mass Spectrometry. *J. Am. Soc. Mass Spectrom.* **1999**, *10*,. 104-111.
(12) Albrethsen, J. Reproducibility in Protein Profiling by MALDI-TOF Mass Spectrometry.*Clin. Chem.* **2007**, *53*, 852–858.
(13) Hamm, G.; Bonnel, D.; Legouffe, R.; Pamelard, F.; Delbos, J. M.; Bouzom, F.; Stauber, J. Quantitative Mass Spectrometry Imaging of Propranolol and Olanzapine Using Tissue Extinction Calculation as Normalization Factor. *J. Proteomics* **2012**, *75*, 4952–4961.
(14) Lemaire, R.; Tabet, J. C.; Ducoroy, P.; Hendra, J. B.; Salzet, M.; Fournier, I. Solid Ionic Matrixes for Direct Tissue Analysis and MALDI Imaging. *Anal. Chem.* **2006**, *78*, 809–819.
(15) Taga, Y.; Iwasaki, Y.; Shigemura, Y.; Mizuno, K. Improved *in vivo* Tracking of Orally Administered Collagen Hydrolysate Using Stable Isotope Labeling and LC–MS Techniques. *J. Agric. Food Chem.* **2019**, *67*, 4671–4678.
(16) Norris, J. L.; Caprioli, R. M. Absolute Quantification of Rifampicin by MALDI Imaging Mass Spectrometry Using Multiple TOF/TOF Events in a Single Laser Shot. *Chem. Rev.* **2013**, *113*, 2309–2342.
(17) Pirman, D. A.; Reich, R. F.; Kiss, A.; Heeren, R. M. A.; Yost, R. A. Quantitative MALDI Tandem Mass Spectrometric Imaging of Cocaine from Brain Tissue with a Deuterated Internal Standard. *Anal. Chem.* **2013**, *85*, 1081–1089.
(18) Sammour, D. A.; Marsching, C.; Geisel, A.; Erich, K.; Schulz, S.; Guevara, C. R.; Rabe, J. H.; Marx, A.; Findeisen, P.; Hohenberger, P.; Hopf, C. Quantitative Mass Spectrometry Imaging Reveals Mutation Status-independent Lack of Imatinib in Liver Metastases of Gastrointestinal Stromal Tumors. *Sci. Rep.* **2019**, *9*, 10698.
(19) Barry, J. A.; Ait-Belkacem, R.; Hardesty, W. M.; Benakli, L.; Andonian, C.; Licea-Perez, H.; Stauber, J.; Castellino, S. Multicenter Validation Study of Quantitative Imaging Mass Spectrometry. *Anal. Chem.* **2019**, *91*, 6266–6274.
(20) Koeniger, S. L.; Talaty, N.; Luo, Y.; Ready, D.; Voorbach, M.; Seifert, T.; Cepa, S.; Fagerland, J. A.; Bouska, J.; Buck, W.; Johnson, R. W.; Spanton, S. A Quantitation Method for Mass Spectrometry Imaging. *Rapid Commun. Mass Spectrom.* **2011**, *25*, 503–510
(21) Prentice, B. M.; Chumbley, C. W.; Caprioli, R. M. Absolute Quantification of Rifampicin by MALDI Imaging Mass Spectrometry Using Multiple TOF/TOF Events in a Single Laser Shot. *J. Am. Soc. Mass. Spectrom.* **2017**, *28*, 136–144.
(22) Benabdellah, F; Touboul, D; Brunelle, A; Laprevote, O. In Situ Primary Metabolites Localization on a Rat Brain Section by Chemical Mass Spectrometry Imaging. *Anal. Chem.* **2009**, *81*, 5557–5560.
(23) Porta, T.; Lesur, A.; Varesio, E.; Hopfgartner, G. Quantification in MALDI-MS Imaging: What Can We Learn from MALDI-Selected Reaction Monitoring and What Can We Expect for Imaging? *Anal. Bioanal. Chem.* **2015**, *407*, 2177–2187.
(24) Gemperline, E.; Rawson, S.; Li, L. Optimization and Comparison of Multiple MALDI Matrix Application Methods for Small Molecule Mass Spectrometric Imaging. *Anal. Chem.* **2014**, *86*, 10030–10035.
(25) Xie, H.; Wu, R.; Hung, Y. L. W.; Chen, X.; Chan, T. W. D. Development of a Matrix Sublimation Device with Controllable Crystallization Temperature for MALDI Mass Spectrometry Imaging. *Anal. Chem.* **2021**, *93*, 6342–6347.
(26) Hong, S.; Tanaka, M.; Yoshii, S.; Mine, Y.; Matsui, T. Enhanced Visualization of Small Peptides Absorbed in Rat Small Intestine by Phytic-Acid-Aided Matrix-Assisted Laser Desorption/Ionization-Imaging Mass Spectrometry. *Anal. Chem.* **2013**, *85*, 10033–10039.
(27) Terahara, N.; Matsui, T.; Fukui, K. Matsugano, K.; Sugita, K. Matsumoto K. Caffeoylsophorose in a Red Vinegar Produced through Fermentation with Purple Sweetpotato. *J. Agric. Food Chem.* **2003**, 9, 2539–2543
(28) Zhang, J. L.; Zhang, G. D.; Zhou, T. H. Metabolism of Ferulic Acid in Rats. *J. Asian Nat. Prod. Res.* **2005**, *7*, 49–58.
(29) Zhao, Z.; Moghadasian M. H. Chemistry, Natural Sources, Dietary Intake and Pharmacokinetic Properties of Ferulic Acid: A Review *Food. Chem.*, **2008**, *109*, 691–702.
(30) Iwao, T.; Inoue, K.; Hayashi, Y.; Yuasa, H.; Watanabe, J. Metabolic Extraction of Nifedipine during Absorption from the Rat Small Intestine. *Drug Metab. Pharmacokin.* **2002**, *17*, 546–553.

(31) Momma, K.; Takao, A. Fetal Cardiovascular Effects of Nifedipine in Rats. *Pediatr. Res.* **1989**, *26*, 442–447.
(32) Rashid, J.; Mckinstry, C.; Renwick, A. G.; Dirnhuber, M.; Waller, D. G.; George, C. F. Quercetin, an *in vitro* Inhibitor of CYP3A, Does Not Contribute to the Interaction between Nifedipine and Grapefruit Juice. *Br. J. clin. Pharmac.* **1993**; *36*: 460–463.
(33) Cornett, D. S.; Duncan, M. A.; Amster, I. Liquid Mixtures for Matrix-Assisted Laser Desorption. *Anal. Chem.* **1993**, *65*, 2608–2613.
(34) Sun, Z.; Findsen, E. W.; Isailovic, D. Atmospheric Pressure Visible-Wavelength MALDI-MS, *Int. J. Mass Spectrom.* **2012**, *315*, 66–73.
(35) Gary, R, P.; Michael, C. F.; Lloyd, M. S. Matrix- Assisted Laser Desorption/Ionization Mass Spectrometry of Synthetic Ooligodeoxyribonucleotides. *Rapid Commun. Mass Spectrom.* **1992**, *6*, 369.
(36) Van de Plas, R.; Yang, J.; Spraggins, J.; Caprioli, R. M. Image Fusion of Mass Spectrometry and Microscopy: A Multimodality Paradigm for Molecular Tissue Mapping. *Nat. Methods* **2015**, *12*, 366–372.
(37) Spraggins, J. M.; Djambazova, K. V.; Rivera, E. S.; Migas, L. G.; Neumann, E. K.; Fuetterer, A.; Suetering, J.; Goedecke, N.; Ly, A.; Van de Plas, R.; Caprioli, R. M. High-Performance Molecular Imaging with MALDI Trapped Ion-Mobility Time-of-Flight (timsTOF) Mass Spectrometry. *Anal. Chem.* **2019**, *91*, 14552–14560.
(38) Wang, X.; Han, J.; Hardie, D. B.; Yang, J.; Pan. J.; Borchers, C. H. Metabolomic Profiling of Prostate Cancer by Matrix Assisted Laser Desorption/Ionization-Fourier Transform Ion Cyclotron Resonance Mass Spectrometry Imaging using Matrix Coating Assisted by an Electric Field (MCAEF). *Biochim. Biophys. Acta.* **2017**, *7*, 755–767.
(39) Schiller, J. Süss, R.; Fuchs, B.; Müller, M.; Petković, M. Zschörnig, O.; Waschipky, H. The Suitability of Different DHB Isomers as Matrices for the MALDI-TOF MS Analysis of Phospholipids: Which Isomer for What Purpose?. *Eur. Biophys. J.* **2007**, *36*, 517–527
(40) Dueñas, M. E.; Carlucci, L.; Lee, Y. J. Matrix Recrystallization for MALDI-MS Imaging of Maize Lipids at High-Spatial Resolution. *J. Am. Soc. Mass Spectrom.* **2016**, *27*, 1575–1578.
(41) Hankin, J. A.; Barkley, R. M.; Murphy, R. C. Sublimation as a Method of Matrix Application for Mass Spectrometric Imaging. *J. Am. Soc. Mass Spectrom.* **2007**, *18*, 1646–1652.
(42) Zaleski, J.; Daszkiewicz, Z.; Kyziol, J. B. Structure of *N*,4-Dinitroaniline and Its Complex with Sulfolane at 85 K; on the Proton Donor-Acceptor Affinity of the Primary Nitramine ($HNNO_2$) Group. *Acta Cryst.* **2002**, *B58*, 109–115.
(43) Bu, R.; Xiong, Y.; Wei, X.; Li, H.; Zhang, C. Hydrogen Bonding in CHON-Containing Energetic Crystals: A Review. *Cryst. Growth Des.* **2019**, *19*, 5981–5997.
(44) Quinn, J. R.; Zimmerman, S. C.; Del Bene, J. E.; Shavitt, I. Does the A·T or G·C Base-Pair Possess Enhanced Stability? Quantifying the Effects of CH···O Interactions and Secondary Interactions on Base-Pair Stability Using a Phenomenological Analysis and ab Initio Calculations. *J. Am. Chem. Soc.* **2007**, *129*, 934–941.
(45) Deegan, R. D.; Bakajin, O.; Dupont, T. F.; Huber, G.; Nagel, S. R.; Witten, T. A. Capillary Flow as The Cause of Ring Stains from Dried Liquid Drops. *Nature*, **1997**, *389*, 827.
(46) Medina, N.; Huth-Fehre, T.; Westman, A. Matrix-Assisted Laser Desorption: Dependence of The Threshold Fluence on Analyte Concentration. *J. Mass Spectrom.* **1994**, *29*, 207–209.
(47) Dreisewerd, K.; Schürenberg, M.; Karas, M.; Hillenkamp, F. Influence of The Laser Intensity and Spot Size on The Desorption of Molecules and Ions in Matrix-Assisted Laser Desorption/Ionization with A Uniform Beam Profile. *Int. J. Mass Spectrom. Ion Processes* **1995**, *141*, 127−148.
(48) Aichler, M.; Walch, A. MALDI Imaging Mass Spectrometry: Current Frontiers and Perspectives in Pathology Research and Practice. *Lab. Investig.* **2015**, *95*, 422–431.
(49) Gessel, M. M.; Norris, J. L.; Caprioli, R. M. MALDI Imaging Mass Spectrometry: Spatial Molecular Analysis to Enable a New Age of Discovery. *J. Proteom.* **2014**, *107*, 71–82.
(50) Caprioli, R. M. Imaging Mass Spectrometry: Enabling a New Age of Discovery in Biology and Medicine Through Molecular Microscop. *J. Am. Soc. Mass Spectrom.* **2015**, *26*, 850–852.
(51) Rzagalinski I, Kovačević B., Hainz N., Meier C., Tschernig T., Volmer DA. Toward Higher Sensitivity in Quantitative MALDI Imaging Mass Spectrometry of CNS Drugs using A Nonpolar Matrix. *Anal. Chem.* **2018**, *90*, 12592−12600.
(52) Rzagalinski, I.; Hainz, N.; Meier, C.; Tschernig, T.; Volmer, D. A. MALDI Mass Spectral Imaging of Bile Acids Observed as Deprotonated Molecules and Proton-Bound Dimers from Mouse Liver Sections. *J. Am. Soc. Mass Spectrom.* **2018**, *29*, 711−722.

Table of Contents (TOC)